WILEY

RESEARCH ARTICLE

Acute tryptophan loading decreases functional connectivity between the default mode network and emotion-related brain regions

Yacila I. Deza-Araujo[1] ⓘ | Philipp T. Neukam[1] ⓘ | Michael Marxen[1] ⓘ | Dirk K. Müller[1] | Thomas Henle[2] | Michael N. Smolka[1] ⓘ

[1]Department of Psychiatry and Neuroimaging Center, Technische Universität Dresden, Dresden, Germany

[2]Institute of Food Chemistry, Technische Universität Dresden, Dresden, Germany

Correspondence
Michael N. Smolka, MD, Section of Systems Neuroscience, Department of Psychiatry and Psychotherapy, Technische Universität Dresden, Würzburger Str. 35, 01187 Dresden, Germany.
Email: michael.smolka@tu-dresden.de

Funding information
TU Dresden; German Academic Exchange Service; Deutsche Forschungsgemeinschaft, Grant/Award Numbers: SFB 940/2, SFB 940/1

Abstract

It has been shown that the functional architecture of the default mode network (DMN) can be affected by serotonergic challenges and these effects may provide insights on the neurobiological bases of depressive symptomatology. To deepen our understanding of this possible interplay, we used a double-blind, randomized, cross-over design, with a control condition and two interventions to decrease (tryptophan depletion) and increase (tryptophan loading) brain serotonin synthesis. Resting-state fMRI from 85 healthy subjects was acquired for all conditions 3 hr after the ingestion of an amino acid mixture containing different amounts of tryptophan, the dietary precursor of serotonin. The DMN was derived for each participant and session. Permutation testing was performed to detect connectivity changes within the DMN as well as between the DMN and other brain regions elicited by the interventions. We found that tryptophan loading increased tryptophan plasma levels and decreased DMN connectivity with visual cortices and several brain regions involved in emotion and affect regulation (i.e., putamen, subcallosal cortex, thalamus, and frontal cortex). Tryptophan depletion significantly reduced tryptophan levels but did not affect brain connectivity. Subjective ratings of mood, anxiety, sleepiness, and impulsive choice were not strongly affected by any intervention. Our data indicate that connectivity between the DMN and emotion-related brain regions might be modulated by changes in the serotonergic system. These results suggest that functional changes in the brain associated with different brain serotonin levels may be relevant to understand the neural bases of depressive symptoms.

KEYWORDS

DMN connectivity, resting state fMRI, serotonin, tryptophan

1 | INTRODUCTION

The brain's default mode network (DMN) has emerged as a landmark in cognitive and affective neuroscience since its first description in 2001 (Raichle et al., 2001). It is now generally accepted that the synchronized activity between its regions might play a critical role for integrating representational information across the cortex (Margulies et al., 2016). Recently, it has been shown that pharmacological challenges may impact the functional architecture of the DMN, especially in regions with elevated receptor density for particular neurotransmitters (e.g., cingulate cortex; Klaassens et al. [2015]).

Specifically, DMN regions receive dense serotonin (5-hydroxytryptamine [5-HT]) innervations (Saulin, Savli, & Lanzenberger, 2012). Serotonergic ascending fibers from the dorsal raphe nucleus project onto the lateral cerebral cortex and the hypothalamus, the basal forebrain, and the amygdala. Further projections from the latter regions continue to the cingulate cortex, the medial cerebral cortex and the hippocampus (Hornung, 2003), which are parts of the DMN (Buckner, Andrews-Hanna, & Schacter, 2008). Presumably as a result of this innervation, changes in the functional coherence of the DMN following serotonergic medication were observed, especially in brain regions involved in mood and attention regulation (Klaassens et al.,

2016, 2015; Posner et al., 2013; Van de Ven, Wingen, Kuypers, Ramaekers, & Formisano, 2013).

Among serotonergic interventions, acute tryptophan challenges are well-established techniques to manipulate the synthesis of 5-HT in the central nervous system in a transitory and marginally invasive manner. Although direct measures of tryptophan influx into the human brain are currently not possible, the effectiveness of these challenges has been demonstrated by several animal studies (Biskup et al., 2012; Grimes, Cameron, & Fernstrom, 2000; Lieben, Blokland, Westerink, & Deutz,, 2004) and indirect measures of 5-HT levels in humans (e.g., CSF; Williams, Shoaf, Hommer, Rawlings, & Linnoila, 1999; Young & Gauthier, 1981). These interventions reduce or enhance the availability of the essential amino acid tryptophan, the dietary precursor of 5-HT in the brain, and thus help to investigate the role of the serotonergic system in the modulation of cognitive functions and mood among others (Lindseth, Helland, & Caspers, 2015; Silber & Schmitt, 2010).

Although simplistic and refined through the years, the hypothesis of a dysfunction in the serotonergic system as a primary factor in the etiology of affective disorders (Cowen & Browning, 2015) has promoted the use of tryptophan challenges in the study of depressive symptomatology (Lindseth et al., 2015). In addition, an aberrant DMN connectivity was found in depressed individuals, establishing a neural model that helps to explain the states of excessive rumination, that is, DMN hyperconnectivity, and deficits in goal-directed behavior, that is, hypoconnectivity between DMN and cognitive control systems, that characterize this disorder (Kaiser, Andrews-Hanna, Wager, & Pizzagalli, 2015). Consequently, DMN changes following tryptophan manipulations might provide relevant clues regarding the origin of depressive symptomatology.

Existing studies investigating the effects of tryptophan depletion on DMN connectivity describe reduced functional connectivity of the precuneus and enhanced functional connectivity of the frontal cortex in healthy (Helmbold et al., 2016; Kunisato et al., 2011) and psychiatric (Biskup et al., 2016) populations. In contrast, tryptophan loading, a less-used intervention, led to greater connectivity between frontal DMN regions and the lateral PFC (Kroes et al., 2014). However, the use of relatively small samples and a single tryptophan condition limits the conclusions that can be drawn from these investigations.

While the effects on 5-HT synthesis obtained after tryptophan challenges seem to be rapid (Biskup et al., 2012; Dingerkus et al., 2012), animal models have shown that low or single doses of SSRIs increase 5-HT concentrations to a level that floods somatodendritic $5-HT_{1A}$ autoreceptors, which in turn may cause a subsequent 5-HT depletion-like state with its corresponding behavioral manifestations (Cools, Roberts, & Robbins, 2008) instead of an expected increase in 5-HT levels. This mechanism of action might explain why DMN changes in healthy subjects after single doses of SSRIs mirror those obtained after tryptophan depletion in posterior parts of the DMN (Helmbold et al., 2016; Klaassens et al., 2015; Kunisato et al., 2011; Van de Ven et al., 2013). On the other hand, the action of serotonergic manipulations on frontal DMN regions seems to be less clear, showing both increases and decreases in connectivity after either SSRIs (Klaassens et al., 2015, 2016) or tryptophan manipulations (Helmbold et al., 2016; Kunisato et al., 2011). Hence, further investigations are still necessary in order to understand how different brain 5-HT levels affect the functional coherence of the DMN.

The aim of our study was to investigate the effects of serotonergic manipulations on the functional architecture of the DMN in healthy subjects following two tryptophan interventions, namely: acute tryptophan depletion (ATD) and acute tryptophan loading (ATL). Both interventions were tested against a balanced condition (BAL), which provided the recommended daily intake of tryptophan for adults (see Experimental procedure). To observe how different brain 5-HT levels may affect the DMN connectivity, we also investigated possible linear relationships between both interventions (ATD–ATL). Based on previous findings and the existing literature, we hypothesized that ATD would decrease the functional connectivity of posterior parts of the DMN (i.e., precuneus and PCC) but increase the connectivity of frontal and medial parts of the DMN (i.e., vmPFC, retrosplenial cortex, and angular gyrus) whereas ATL would have opposite effects. The methodology used in this study also allowed us to investigate connectivity changes between the DMN and other brain regions following each tryptophan manipulation (i.e., voxel-to-network connectivity). Additionally, we used similar behavioral measures as previous studies that reported more impulsive choices as well as higher anxiety and depression levels after ATD, and increasing sleepiness after ATL (Dougherty, Richard, James, & Mathias, 2010; Lindseth et al., 2015; Silber & Schmitt, 2010). Finally, we investigated possible associations between functional connectivity changes and these behavioral measures.

2 | MATERIALS AND METHODS

2.1 | Participants

One hundred and twelve healthy participants completed the three sessions of the study. Of these, we discarded five participants who received accidentally the same mixture in all sessions, four participants with excessive movement during the resting-state scan (see section on "Image preprocessing"), four participants with structural brain anomalies (e.g., cysts, enlarged ventricles) detected by a neuroradiologist, two participants who did not complete one resting state scan and 12 participants with limited brain coverage or scanner artifacts in one or all resting-state sessions. Therefore, data from 85 participants (41 females; M_{age} = 32.68 years, $SD_{age} \pm 5.81$, range = 21–42) were analyzed in this study. These participants form part of the sample already reported by Neukam et al. (2018). The detailed recruitment process is described in the Supporting Information Material S1.

Participants gave written informed consent and received monetary compensation for their participation. The study protocol was approved by the local ethics committee of the Technische Universität Dresden and was in accordance with national legislation and the Declaration of Helsinki.

2.2 | Experimental procedure

Participants took part in three sessions and received one of the following drinks: acute tryptophan depletion (ATD), balanced (BAL), or acute tryptophan loading (ATL) in a randomized, double-blind, placebo-controlled (BAL), crossover study, with at least 1 week between sessions (elapsed

days between sessions: M = 23, SD = 25). The dose of amino acids in the mixtures was adjusted to participant's body weight (Dingerkus et al., 2012; Moja et al., 1988) and contained the same amount of large neutral amino acids (LNAA) but differed in the amount of tryptophan. In the ATD condition, tryptophan was completely absent, the BAL condition contained 7 mg/kg body weight (equivalent to the recommended daily allowance for adults; Richard et al., 2009) and the ATL condition contained 70 mg/kg body weight. The dose of large neutral amino acids (LNAA) was constant for every participant across sessions: L-phenylalanine (132 mg/kg), L-leucine (132 mg/kg), L-isoleucine (84 mg/kg), L-methionine (50 mg/kg), L-valine (96 mg/kg), L-threonine (60 mg/kg), and L-lysine (96 mg/kg). To maximize the effects of the intervention, we provided a list of low-protein food that the participants were allowed to have for dinner and told them to fast overnight before each experimental day. Participants arrived either at 8.30 am or 10.30 am, received instructions about the study procedure and the possible side-effects of the intervention (e.g., sleepiness, drowsiness, nausea, and vomiting) and drank the assigned mixture prepared by an independent experimenter who did not conduct the session. Additional details about the experimental procedure are provided in Supporting Information Material S2.

2.3 | Biochemical measures

A venous catheter (Braunüle®) was inserted in the participant's arm at the beginning of each session in order to draw blood samples in tubes (Sarstedt, Germany) with ethylenediaminetetraacetic acid (EDTA) at four time points (T0 = baseline, T1 = 1 hr, T2 = 3 hr, and T3 = 6 hr after ingestion of the mixture) to measure the concentrations of tryptophan and LNAA in blood plasma. Blood samples were immediately centrifuged at 4,000g and 4 °C for 10 min and 1 mL plasma was stored in two Eppendorf capsules in a −81 °C fridge. Plasma analyses for the concentrations of tryptophan and LNAA were conducted at the Department of Chemistry and Food Chemistry of the Technische Universität Dresden as described in Henle, Walter, Krause, and Klostermeyer (1991). Complete blood samples from 71 participants were available for analysis.

The ratio of tryptophan to the sum of the other LNAA (TRP/$\sum$LNAA) in the peripheral blood at each time point was calculated as the best estimate of the intervention effects in each session (Dingerkus et al., 2012). For statistical analyses, the area under the curve (AUC) was computed using the four time points. Before calculating the AUC, all four time points were normalized by subtracting the values of T0 from all time points, thereby accounting for interindividual differences in baseline blood levels. These AUC scores were entered into a repeated-measures ANOVA.

2.4 | Behavioral assessment

Statistical analyses were conducted using SPSS for Windows (release 22.0, IBM Corp., Armonk, IL, USA). Participants completed an extensive behavioral assessment and several self-report questionnaires. The questionnaires reported in this manuscript are the State–Trait Anxiety Inventory (STAI-State; Spielberger, 1983), the Karolinska Sleepiness Scale (KSS; Akerstedt & Gillberg, 1990) and a 9-item Visual Analogue

Scale (VAS: heightened, excited, balanced, depressed, lethargic, activated, sad, relaxed, stressed [In-house assessment, ZI, Mannheim, Germany]). These questionnaires were applied in the order mentioned above at the four time points of the session. Additionally, we assessed impulsive choice using three tasks of the Value-Based Decision-Making battery (see Pooseh, Bernhardt, Guevara, Huys, & Smolka, 2017 for a complete description). Briefly, risk aversion for gains and risk seeking for losses were assessed using probability discounting for gains and losses, respectively. In these tasks, participants needed to choose between a sure amount that they could win or lose and the probability of winning/losing a larger amount of money (e.g., 75% probability of winning €5 or winning €2 for sure, or a 50% probability of losing €8 or losing €3 for sure). The resulting main discounting parameters from these tasks (k) were log-transformed in order to approximate them to a normal distribution. Finally, loss aversion was assessed with a mixed gambles task. In this task, participants received a credit of €10 at the beginning of the game and then needed to decide whether to accept or reject an offer with a 50/50 chance of either gaining one amount of money or losing another amount (e.g., refusing to gamble or accepting a gamble that offered either winning €15 or losing €8). These three tasks were administered at a single time point after the fMRI session. Due to missing data the number of complete behavioral datasets ranged from 82 to 85. Other behavioral and cognitive measures as well as demographic information were acquired (see Neukam et al. (2018) and Supporting Information Material S3). The study design including the number of participants in each session and condition and a schematic overview of one study session are depicted in Figure 1.

In order to test intervention effects (ATD and ATL vs. BAL) and effects between interventions (ATD vs. ATL) on the three behavioral ratings, we subtracted the scores obtained at baseline (T0) from the scores obtained before the scan session (T2) and performed a repeated-measures ANOVA with the resulting scores. Results were Bonferroni-corrected for 14 comparisons. If the F-test indicated significant differences, post-hoc paired t-tests were performed to determine directionality of the effects.

2.5 | MR data acquisition

All fMRI sessions were carried out 3 hr after the ingestion of the mixtures because previous research (Dingerkus et al., 2012) and our pilot tests showed after this time, the lowest and highest tryptophan peaks in ATD and ATL, respectively. The resting-state fMRI sequence was performed after a decision-making task and a short break. fMRI data were collected on a 3 Tesla whole-body MRI Scanner Magnetom Trio Tim (Siemens Healthcare GmbH, Erlangen, Germany) equipped with a 32 channel head coil using a single-shot gradient echo-planar imaging (EPI) sequence with repetition time (TR) of 2.41 s, an echo time (TE) of 25 ms, a flip angle of 81°, 42 2 mm-thick slices and 1 mm slice gap, field of view of 192 × 192 mm^2 with a matrix size of 64 × 64, 3 mm isotropic resolution, and a bandwidth of 2,112 Hz/Px. A total of 150 resting-state volumes were acquired, tilted slightly from axially to coronal to be parallel to the anterior/posterior commissural line. For registration purposes, a T1-weighted high-resolution anatomical scan was acquired with a 3D magnetization prepared-rapid gradient echo
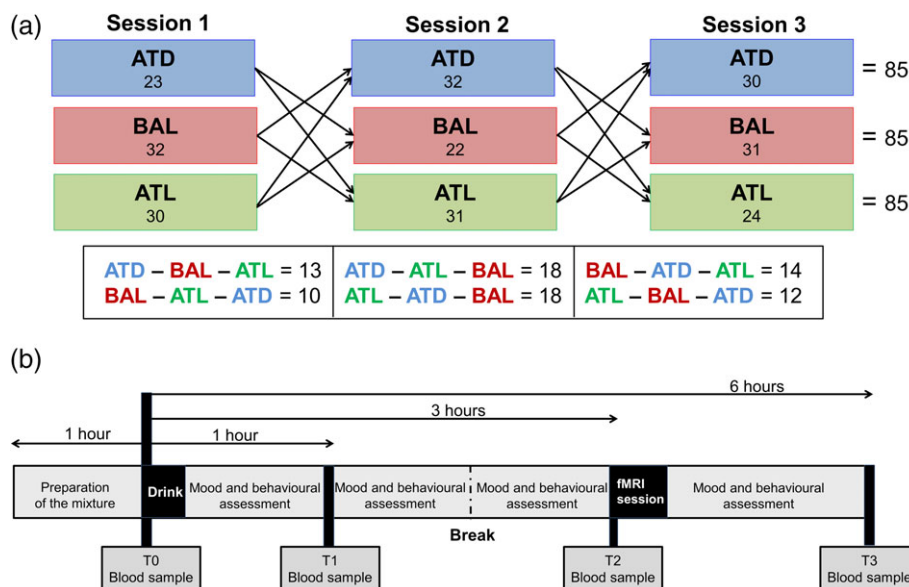
FIGURE 1 Study design. Part a shows the study design with the cross-over randomization of the tryptophan interventions (ATD, acute tryptophan depletion; BAL, balanced; ATL, acute tryptophan loading), the final number of participants for each intervention and session (N = 85) and the number of participants in each possible order of interventions. Part B shows the timeline of a study session. The mixture was prepared 1 hr before the participant arrived. At T0, the first blood sample was taken as a baseline measure of tryptophan plasma concentrations, followed by the ingestion of the mixture and mood and behavioral assessments. Additional blood samples were taken 1, 3, and 6 hr after the ingestion of the mixture. The fMRI session was carried out 3 hr after the drink [Color figure can be viewed at wileyonlinelibrary.com]

(MP-RAGE) sequence (TR = 1.90 s, TE = of 2.26 ms, TI = 900 ms, flip angle of 9°, FOV = 256 × 256 mm^2, 176 slices, 1 mm × 1 mm × 1 mm voxel size with slice thickness of 1 mm and 200 Hz/Px bandwidth). Participants were given earplugs for noise protection and foam pads to minimize head movement. They were instructed not to think about anything in particular and to lie as still as possible while fixating on a black crosshair presented on the center of a white screen. An eye-tracking camera was used to monitor the participants and to ensure that they remained awake during the whole resting-state session.

2.6 | Image preprocessing

For each participant, framewise displacement (FD: a sum of the absolute values of the temporal derivatives of the volume-by-volume changes in the translational and rotational realignment estimates; Power, Barnes, Snyder, Schlaggar, & Petersen, 2012), was calculated on the raw data prior to any preprocessing step using the tool fsl_motion_outliers. Four participants with more than 10% of volumes over a FD of 0.5 mm were excluded from the analysis (Deza Araujo et al., 2018). The resting-state fMRI data were preprocessed using the Functional Magnetic Resonance Imaging of the Brain (FMRIB) Software Library (FSL Version 5.0.9, www.fmrib.ox.ac.uk/fsl; Jenkinson, Beckmann, Behrens, Woolrich, & Smith, 2012). The first four volumes of each functional scan were discarded to allow for magnetic equilibration, resulting in 146 volumes per subject and intervention. Preprocessing steps included motion correction with MCFLIRT, brain extraction of the EPI data with BET, spatial smoothing with a 5 mm Gaussian kernel of full-width at half maximum, ICA-based denoising using ICA-AROMA (Pruim et al., 2015) and high-pass temporal filtering of 0.01 Hz. Registration was applied on the denoised functional data using the registration parameters derived from nonsmoothed and

nonfiltered data. For registration, individual resting-state images were aligned to their corresponding T1-weighted image using a boundary-based registration algorithm (BBR; Greve & Fischl, 2009). The T1-weighted images were registered to MNI space (MNI152; 2 mm × 2 mm × 2 mm spatial resolution) using a nonlinear registration implemented in FNIRT (warp resolution: 10 mm). The same transformation was applied to the filtered EPI images. After this process, all images were visually inspected in order to ensure accuracy of the registration.

2.7 | Generation and analysis of the default mode network

We used a template-based approach, which has been validated by previous studies (Klaassens et al., 2015, 2016) and reliably provides spatial maps of established large-scale brain networks. Briefly, we used the 10 templates from Smith et al. (2009) to derived the networks identified in more than 1,600 studies. These templates included: high, medial and lateral visual networks, default-mode network, cerebellar network, sensorimotor network, auditory network, cingulo-opercular network, right and left fronto-parietal networks (see Supporting Information Figure S2; Smith et al., 2009). To obtain an individual representation of each network, we used a dual regression analysis (Beckmann, Mackay, Nicola, & Smith, 2009). Here the templates were linearly regressed against the functional data of each subject, resulting in individual time courses (spatial regression) for each one of the 10 networks. These time courses were normalized and then regressed against the corresponding functional datasets (temporal regression) to estimate 10 subject-specific voxel-to-network spatial maps for each subject and pharmacological condition. Additional individual mean time courses from white matter, cerebrospinal fluid and the six subject-specific motion parameters were added

during the last stage of the dual regression to remove sources of spurious variance and residual motion (see Supporting Information Material S4). As a multivariate approach, this dual regression procedure allowed the estimation of a "clean" representation of the DMN in which temporal and spatial signals that this network shares with other networks, were removed. In the dual regression approach, the estimated maps do not depend on the initial subject-specific major Eigenspaces (PCA) and therefore, may lie outside the network's boundaries (Beckmann et al., 2009). The voxel-wise regression coefficients contained in the resulting spatial maps represent the synchronization between BOLD temporal dynamics at a given voxel and the mean BOLD time courses of a specific network. The strength of the voxel-to-network connectivity is given by the value of these coefficients (Klaassens et al., 2015, 2016). Only the spatial maps representing the DMN were used in the higher-level analysis (85 subjects × 3 interventions = 255 DMN maps).

Due to the unknown distribution of the data, nonparametric testing was used for group-level analyses. To delineate the effects of intervention on the DMN, a repeated-measures ANOVA was performed, with "intervention" (ATD, BAL, and ATL) as a within-subject factor. We used Faster Permutation Inference as implemented in Permutation Analysis of Linear Models – PALM version 99a (Winkler, Webster, Vidaurre, Nichols, & Smith, 2015), with 500 - permutations and a tail approximation procedure which fits a Pareto distribution to the tail of the distribution used for correction of the *p*-values (Winkler, Ridgway, Douaud, Nichols, & Smith, 2016). Exchangeability blocks were specified in the model for allowing permutations to happen within subjects (Winkler et al., 2015). We implemented directional contrasts to compare if the within DMN connectivity and the voxel-to-network connectivity were stronger or weaker after a given intervention with respect to baseline levels (ATD > BAL, BAL > ATL, ATD < BAL, BAL < ATL) and between both interventions (ATD < ATL, ATD > ATL). Results were family-wise error (FWE) corrected at 0.05 using Threshold-Free Cluster Enhancement – TFCE, a method that generates a voxel-wise output image in which the values represent the amount of cluster-like local spatial support (Smith & Nichols, 2009). Further FWE correction over the six tested contrasts was performed, using the option "corrcon" implemented in PALM (Winkler, Webster, et al., 2016), which takes into account the dependencies that might exist between contrasts. These comparisons of subject-specific maps indicated which brain areas (within or outside the DMN map) are stronger connected to the DMN under one condition with respect to the other.

Additionally, we tested potential repetition effects. To this aim, a repeated measures ANOVA with "intervention" (ATD, BAL, and ATL) as a within-subjects factor and "intervention order" (i.e., the six possible order combinations of the interventions; see Figure 1) as between-subject factor, was used. A significant interaction between these two factors would indicate that the observed effects on DMN connectivity are driven by the repetition of the resting-state scan and not solely by a given intervention.

Due to postulated gender differences in brain 5-HT metabolism (Nishizawa et al., 1997), we explored whether gender moderates the effects of the tryptophan interventions. To this end, a third repeated-measures ANOVA was included, with "intervention" as a within-subject factor and "gender" (males, females) as a between-subject factor. These additional models were also tested using 500 permutations, with a tail approximation as implemented in PALM, yielding voxel-wise maps identified with TFCE and corrected at 0.05.

Finally, we compared the mean FD measures in a repeated measures model to test whether in-scanner motion differed between interventions or sessions.

2.8 | Analyses of brain-behavior associations

To determine potential brain-behavior associations, we performed Pearson correlations between the behavioral scores and the brain regions with significant intervention effects on DMN connectivity. Specifically, the difference of regional parameter estimates between two interventions (e.g., BAL – ATL) was correlated with their corresponding difference in behavioral scores (e.g., $KSS_{BAL} - KSS_{ATL}$).

3 | RESULTS

3.1 | Effects of intervention on blood plasma levels of tryptophan and $\sum$LNAA

To test the effects of our interventions in the peripheral blood, TRP/$\sum$LNAA AUC scores and free tryptophan measures were calculated. Significant main intervention effects were found in the measures of free tryptophan in peripheral blood ($F_{2,142} = 235.52$; $p = 1.76 \times 10^{-28}$) and in the TRP/$\sum$LNAA AUC scores ($F_{2,142} = 334.30$; $p = 1.15 \times 10^{-33}$). Contrast analyses revealed significant increases for free tryptophan from ATD to BAL ($F_{1,70} = 65.44$; $p = 1.13 \times 10^{-11}$) and from BAL to ATL ($F_{1,70} = 174.55$; $p = 8.23 \times 10^{-21}$). In the same manner, contrasts analysis for TRP/$\sum$LNAA AUC scores revealed significant increases from ATD to BAL ($F_{1,70} = 67.40$; $p = 7.5 \times 10^{-12}$) and from BAL to ATL ($F_{1,70} = 250.28$; $p = 8.2 \times 10^{-25}$). Graphic representations of these effects are displayed in Figure 2. Detailed results of this analysis as well as other measures (free tryptophan and TRP/$\sum$LNAA) are provided in Supporting Information Table S1.

Finally, neither gender nor intervention order had any effect on tryptophan plasma measures (all *p*s > 0.2).

3.2 | Effects of intervention on mood, vigilance, and impulsive choice

None of the behavioral scores survived Bonferroni correction for 14 comparisons. For completeness, we reported uncorrected *p*-values (main effects of intervention and pair-wise comparisons) in Table 1.

3.3 | Effects of intervention on DMN connectivity

Compared with the control condition (BAL), acute tryptophan loading (ATL) reduced significantly the DMN functional connectivity in bilateral medial prefrontal regions ($p_{FWE} = 0.03$). The same intervention reduced the functional connectivity between the DMN and clusters located in the putamen ($p_{FWE} = 0.02$), subcallosal cortex ($p_{FWE} = 0.03$),
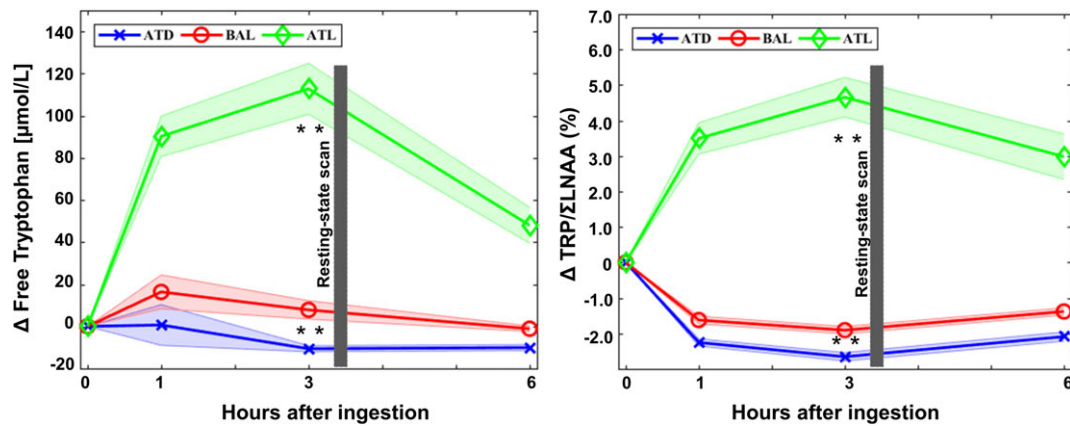
FIGURE 2 Pharmacokinetics of the acute tryptophan intervention: In both graphs, the x axis displays the four time points of blood sampling. On the left graph, the y axis displays the plasma levels of free tryptophan. On the right graph, the ratio of tryptophan to the sum of the other large neutral amino acids (TRP/$\sum$LNAA) is shown. The resting-state scan was carried out after a decision-making task, 3.5 hr after the ingestion of the mixture. The abbreviations are acute tryptophan depletion (ATD), balanced (BAL), and acute tryptophan loading (ATL). The shaded areas indicate bias-corrected and accelerated (BCa) 95% confidence intervals. The graph includes complete data from 71 participants. ** $p < 0.0001$ [Color figure can be viewed at wileyonlinelibrary.com]

left thalamus (p_{FWE} = 0.03), and bilateral occipital regions (p_{FWE} = 0.02 and 0.04). All these connectivity changes were unrelated to variations in behavioral scores (all ps > 0.20). Cluster sizes and summary statistics for the significant results are presented in Table 2. A graphical representation of all intervention effects on the significant regions is presented in Figure 3.

Compared with the control condition (BAL), acute tryptophan depletion (ATD) numerically decreased the DMN connectivity with small clusters in the left middle temporal gyrus (k = 42) and the right orbitofrontal cortex (k = 7). Importantly, these marginal effects did not survive correction for the six contrasts of interest (p_{FWE} = 0.30; Supporting Information Table S2).

No significant differences in DMN connectivity were found between both interventions (ATD vs. ATL).

Regarding possible confounders or moderators, framewise displacement analyses revealed no differences in-scanner motion between interventions or session (all ps > 0.10). Moreover, no interaction between intervention order and interventions were found, indicating that the repetition of the resting-state scan did not affect DMN connectivity. No significant gender-by-intervention interaction on DMN connectivity could be found, indication that interventions had comparable effects for males and females.

4 | DISCUSSION

This study is the first to use both, tryptophan depletion and loading, together with a control condition to manipulate brain 5-HT levels and

TABLE 1 Summary statistics of the difference between T2 (before the scan session) and T0 (baseline) for the behavioral assessment in each tryptophan intervention

Test	ATD Mean (SD)	ATD–BAL p-value	BAL Mean (SD)	BAL–ATL p-value	ATL Mean (SD)	ATD–ATL p-value	Main effects p-value
STAI-G X1-state	1.12 (5.00)	0.85	1.36 (5.40)	0.80	1.61 (4.11)	0.62	0.88
KSS	1.41 (2.08)	0.27	1.17 (1.96)	0.006*	1.86 (2.13)	0.19	0.04*
VAS-heightened (mm)	−6.83 (24.83)	0.94	−7.03 (24.56)	0.31	−3.64 (17.56)	0.35	0.52
VAS-excited (mm)	−9.32 (28.92)	0.23	−5.01 (19.41)	0.43	−8.03 (23.52)	0.68	0.49
VAS-balanced (mm)	−0.44 (28.33)	0.74	−1.80 (24.25)	0.40	−5.69 (30.81)	0.25	0.49
VAS-depressed (mm)	2.04 (16.63)	0.06	7.05 (21.80)	0.32	4.07 (16.36)	0.28	0.14
VAS-lethargic (mm)	14.02 (28.41)	0.52	11.15 (27.61)	0.28	16.04 (29.43)	0.65	0.55
VAS-activated (mm)	−10.68 (22.15)	0.70	−9.38 (19.06)	0.63	−11.08 (24.43)	0.91	0.87
VAS-sad (mm)	3.55 (13.52)	0.30	1.41 (13.30)	0.62	2.68 (18.31)	0.55	0.55
VAS-relaxed (mm)	−6.20 (21.79)	0.37	−3.79 (24.80)	0.02*	−12.74 (26.46)	0.12	0.06
VAS-stressed (mm)	−1.80 (13.54)	0.03*	5.52 (24.12)	0.48	3.73 (15.83)	0.01*	0.04*
PDG$_{logk}$	0.37 (0.85)	1.00	0.31 (1.04)	1.00	0.23 (0.82)	0.51	0.38
PDL$_{logk}$	−0.15 (0.99)	0.28	−0.38 (1.25)	0.35	−0.33 (1.52)	0.63	0.34
MG$_\lambda$	143 (0.98)	1.00	1.48 (1.13)	1.00	1.44 (1.13)	1.00	0.89

None of the comparisons survived Bonferroni correction for 14 tests. Asterisks indicate ps < 0.05, uncorrected for multiple comparisons.
N = 82–85.
STAI-G X1, state–trait anxiety inventory–state, scale X1; KSS, Karolinska sleepiness scale; VAS, visual analogue scale, mm, millimeters; PDG, probability discounting gains (k on log scale); PDL, probability discounting losses (k on log scale); MG, mixed gambles (lambda).

TABLE 2 Brain regions that showed significant decreases in functional connectivity to the DMN under ATL compared with BAL

Brain regions	Cluster size (voxels)	t-values	p-values	MNI coordinates (COG)		
				X	Y	Z
Right putamen	1,058	4.41	0.02	20	10	−2
Left frontal orbital cortex	349	4.69	0.02	−30	18	−14
Left subcallosal cortex	153	4.09	0.03	−2	28	−26
Left frontal medial cortex	118	4.29	0.03	−12	44	−10
Right frontal orbital cortex	108	4.29	0.03	38	34	0
Left thalamus	96	4.53	0.03	−10	−2	4
Left occipital pole	80	5.54	0.02	−2	−92	4
Right frontal medial cortex	49	4.42	0.03	14	44	−10
Left frontal pole	41	3.83	0.04	−36	44	−8
Left frontal pole	16	4.14	0.04	−14	44	−24
Right middle frontal gyrus	14	4.13	0.04	36	32	26
Right middle frontal gyrus	11	4.02	0.04	34	24	22
Right occipital pole	10	4.34	0.04	14	−90	10
Left thalamus	10	3.73	0.04	−10	−12	−2

Voxel dimensions = 2 × 2 × 2 mm. Peak t-values within cluster are uncorrected. The p-values are FWE-corrected and adjusted for the six comparisons performed. MNI coordinates represent the center of gravity (COG). Brain areas were identified using the Harvard–Oxford Cortical and Subcortical Structural Atlases.

investigate related changes in DMN functional connectivity in a large cohort of healthy adults. We found that, compared with the control condition (BAL), higher brain 5-HT levels (ATL) decreased the functional connectivity within the DMN and between this network and other brain regions. Contrary to previous findings, lower brain 5-HT levels (ATD) did not yield any significant changes on DMN connectivity. Finally, behavioral measures of mood, sleepiness, vigilance, and impulsive choice were neither strongly affected by our interventions nor related to any DMN connectivity change.

In partial agreement with our hypotheses, higher brain 5-HT levels (ATL) resulted in lower functional connectivity within anterior regions of the DMN (i.e., bilateral medial frontal cortex) but did not increase the functional connectivity of posterior DMN regions. Moreover, the same intervention decreased the functional connectivity between the DMN and the middle frontal gyrus, left frontal pole, and bilateral orbitofrontal cortex. Frontal DMN regions are involved in emotion regulation, introspection and future thinking (Buckner et al., 2008), processes that have a close relationship with serotonergic function and are generally affected in mood disorders (Dainer-Best, Disner, McGeary, Hamilton, & Beevers, 2018; Meneses & Liy-Salmeron, 2012). Similarly, the dense serotonergic innervation of the orbitofrontal cortex indicates that an adequate 5-HT modulation of this area is crucial for behavioral flexibility and regulation of emotional responses (Roberts, 2011). Given the anatomical proximity and the existing connections between the orbitofrontal cortex and the frontal hub of the DMN (i.e., medial prefrontal cortex; Kahnt, Chang, Park, Heinzle, & Haynes, 2012), serotonergic-induced changes in the functional connectivity of these regions may be relevant to understanding, for example, the mood improvements observed after administration of serotonergic medications.

In the same way, higher brain 5-HT levels (ATL) reduced the connectivity between the DMN and the thalamus and putamen. These structures form part of the limbic–cortical–striatal–pallidal–thalamic circuits (LCSPT), which are primarily involved in emotional processing,

affect regulation and are also implicated in the pathophysiology of mood disorders (Drevets, Price, & Furey, 2008; Greicius et al., 2007). Moreover, PET studies have revealed high serotonin synthesis capacity rates in these areas (Okazawa, Leyton, Benkelfat, Mzengeza, & Diksic, 2000; Saulin et al., 2012), indicating their susceptibility to different 5-HT levels.

The decreased connectivity between the DMN and a cluster located in the subcallosal cortex following ATL deserves special attention. The subcallosal cortex comprises the adjacent ventromedial PFC and Brodmann areas 24 and 25 (Vogt, Nimchinsky, Vogt, & Hof, 1995) and plays a fundamental role in affective valuation of stimuli and expression of negative emotions (Drevets, Savitz, & Trimble, 2008). Functional and structural changes in the subcallosal cortex and its adjacent areas are observed in mood and depressive disorders (Drevets, Savitz, et al., 2008). Furthermore, this area exhibits high densities of 5-HT transporters and 5-HT$_{1A}$ receptors (Varnas, Halldin, & Hall, 2004), which may enhance its susceptibility to serotonergic manipulations (Talbot & Cooper, 2006). An increased functional connectivity between the DMN and the subgenual prefrontal cortex (sgPFC), the caudal portion of the subcallosal area, is a common finding in depressive disorders (Berman et al., 2011; Greicius et al., 2007). In addition, a recent model proposed that this hyperconnectivity may explain depressive rumination by means of a two-system interaction: the DMN that brings in self-referential processes and the sgPFC that provides emotional loading to these processes (Hamilton, Farmer, Fogelman, & Gotlib, 2015).

An elevated connectivity of the DMN is consistently reported in depression (Berman et al., 2011; Greicius et al., 2007; Hamilton et al., 2011; Lois & Wessa, 2016; Sheline et al., 2009; Ye et al., 2015) and individuals at high risk for depression (Posner et al., 2016), illustrating potential neural signatures of disrupted self-referential processing and poor impulse control (Kaiser, Andrews-Hanna, Wager, & Pizzagalli, 2015), functions that are closely related to serotonergic activity (Cha et al., 2018; Dainer-Best et al., 2018). In this light, serotonergic
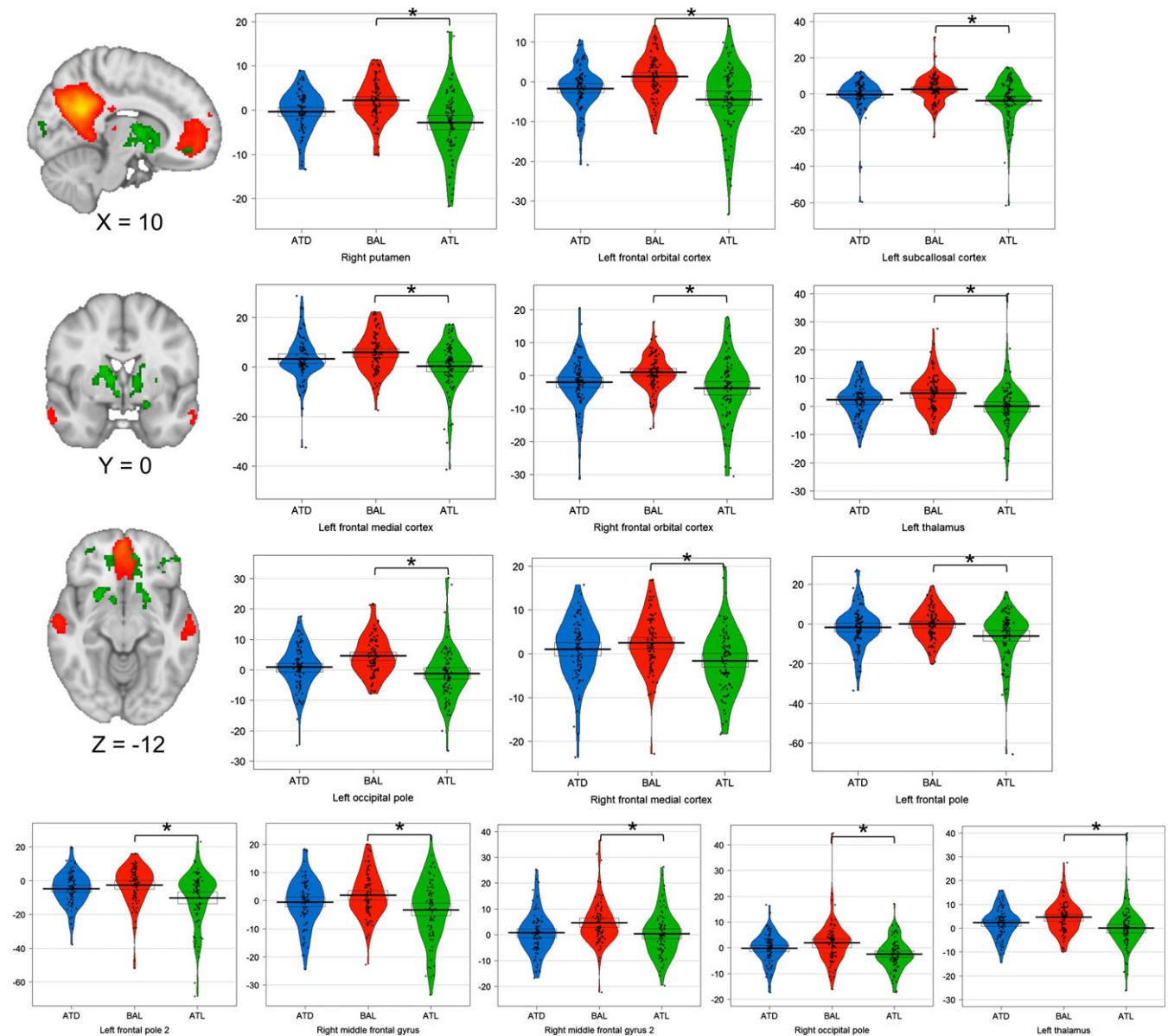
FIGURE 3 Changes in DMN functional connectivity following tryptophan manipulations. The image slices on the left side show the spatial map of the DMN (precuneus, PCC, mPFC, retrosplenial cortex, and hippocampus) as identified by Smith et al. (2009) displayed in red-orange. The clusters with decreased functional connectivity to the DMN after acute tryptophan loading (ATL) are displayed in green colors. MNI coordinates are presented below each image. Images are displayed in radiological orientation (left = right). The plots represent the distribution of the parameter estimates (in arbitrary units) of the brain regions that were affected by the tryptophan manipulations (as shown in Table 2). Horizontal lines on the plots represent means and 95% confidence intervals. *$p < 0.05$, FWE corrected and adjusted for six comparisons performed [Color figure can be viewed at wileyonlinelibrary.com]

manipulations such as antidepressant agents, were found to normalize the elevated DMN connectivity in depressed patients (Posner et al., 2013) and, similar to our findings, decrease the connectivity between DMN regions and subcortical regions in healthy individuals (McCabe & Mishor, 2011), pointing to a plausible neural substrate of depressive symptoms that can be targeted by medication.

In contrast to the effects of ATL on DMN connectivity and previous studies (Biskup et al., 2016; Helmbold et al., 2016; Kunisato et al., 2011), depleting tryptophan yielded only small effects that failed to reach statistical significance. Furthermore, these effects were numerically in the same direction as ATL, that is, if anything ATD slightly decreased connectivity to the DMN.

While our blood measures indicated that ATD significantly lowered plasma tryptophan levels, the lack of robust neural effects may arise from differences in 5-HT stores among our participants or the presence of adaptive brain processes (Young, 2007) that might prevent significant decreases of brain 5-HT in our healthy individuals compared with psychiatric populations (Biskup et al., 2016). Furthermore, methodological differences may also explain why others have reported ATD effects. For example, seed-based approaches provide more power due to strong a priori hypotheses regarding the functional connectivity of the seed region and, therefore, capture more subtle connectivity changes (Eisner et al., 2017). Similarly, other ATD studies use resting-state data but analyze measures, like fractional amplitude

of low-frequency fluctuation (ALFF; Kunisato et al., 2011), that do not quantify functional connectivity (Di et al., 2013). In addition, we suspect that ATD might have smaller effects than found by previous small studies, which leads to an overestimations of effect sizes (Fanelli, Costas, & Ioannidis, 2017). In contrast, our study was performed in a larger sample (n = 85), which provided sufficient power ($1 - \beta = 0.80$) to detect small- to medium- sized effects at the behavioral and network level ($\alpha = 0.05$; $dz = 0.34$) and medium-sized effects at the voxel level ($\alpha = 0.001$; $dz = 0.50$) (Faul, Erdfelder, Lang, & Buchner, 2007), but still ATD effects were not evident. Lastly, we acknowledge that all these interpretations are speculative and certainly merit future in-depth investigation.

At the behavioral level, none of our measures showed significant changes after correction for multiple testing. Regarding the effects of ATD on mood and anxiety, decreases in these scores are mostly reported in depressed or recovered depressed patients, perhaps reflecting a selective vulnerability of the serotonergic system (Fusar-Poli et al., 2006). In addition, depressed patients might also exhibit associations between mood scores and functional connectivity strengths (Posner et al., 2013; Wang et al., 2015; Zhu et al., 2012), in which symptomatic improvements are correlated with reductions in functional connectivity (Wang et al., 2015). In a similar manner, the effects of ATL on these measures may depend on the initial state of the serotonergic system of the individuals. For example, large doses of tryptophan during the daytime may have calming effects in healthy adults but reduce sleep latency and increase subjective ratings of sleepiness in individuals with sleep disturbances (Hartmann, 1982; Silber & Schmitt, 2010). Since we investigated healthy volunteers, it is not surprising that these changes and associations were not statistically reliable in our study. Lastly, although the serotonergic system is involved in the expression of impulsive behaviors (Miyazaki, Miyazaki, & Doya, 2012), our measures of impulsive choice were neither affected by any intervention nor related to functional connectivity changes. Behavioral analyses of this lab support these observations, showing that impulsive choice is not affected by transient changes of tonic 5-HT, but modulated by individual differences in the serotonergic system (Neukam et al., 2018). Nevertheless, our results highlight the role of higher 5-HT brain synthesis as a modulator of the connectivity between the DMN and brain regions involved in emotion processing. One might speculate that diminished serotonergic function in these areas leads to a hyperconnectivity with the DMN and therefore, promotes depressogenic cognition, but caution is warranted due to the known neurobiological differences between depressed patients and healthy individuals and the distributed nature of depression (Pandya, Altinay, Malone, & Anand, 2012).

4.1 | Limitations

Our study has some limitations. First, it has been shown that short scan lengths impact the reliability of the resting-state data across sessions (Birn et al., 2013), which at the same time, reduces the statistical power and allows the detection of only large effect sizes. Future studies might use improved scanning protocols including longer scanning times (e.g., 9–12 min; (Birn et al., 2013)) and accelerated EPI sequences with much shorter TRs (i.e., multiband) which may yield more stable estimates of connectivity strengths, allowing the detection of smaller effects that were not evident in our study (e.g., ATD). In addition, study designs with pre- and post-intervention scans would provide a more stable baseline against which the conditions of interest can be compared. Second, the resting state scan was performed after a decision-making task and a short break (about 2 min). Therefore, possible carry-over effects from the previous task cannot be ruled out. To discard these potential confounds, well-tailored studies entirely dedicate to investigate resting-state activity are encouraged. Finally, despite the extended use of tryptophan challenges for more than 40 years up to now, the specificity of their action on the serotonergic system remains a matter of debate (Crockett et al., 2012; Van Donkelaar et al., 2011). Therefore, further animal and human research is still needed to draw stronger conclusions about the impact of tryptophan challenges on brain 5-HT levels.

5 | CONCLUSION

To sum up, our study is the first to use both ATD and ATL, together with a baseline condition in the same subjects to shed light on acute connectivity changes of the DMN following serotonergic manipulations. Our results expand a large body of ongoing research regarding the serotonergic modulation of the DMN (Biskup et al., 2016; Helmbold et al., 2016; Klaassens et al., 2015; Kunisato et al., 2011; Posner et al., 2013; Van de Ven et al., 2013). More specifically, our data support the notion of decreased connectivity between the DMN and emotion-related regions after increasing brain 5-HT levels and suggest that these functional changes represent a key feature for the understanding of the neural basis of depressive symptomatology.

ORCID

Yacila I. Deza-Araujo https://orcid.org/0000-0002-2624-077X
Philipp T. Neukam https://orcid.org/0000-0002-9442-0043
Michael Marxen https://orcid.org/0000-0001-8870-0041
Michael N. Smolka https://orcid.org/0000-0001-5398-5569

REFERENCES

Akerstedt, T., & Gillberg, M. (1990). Subjective and objective sleepiness in the active individual. *International Journal of Neuroscience*, *52*(1-2), 29–37.

Beckmann, C. F., Mackay, C. E., Nicola, F., & Smith, S. M. (2009). Group comparison of resting-state FMRI data using multi-subject ICA and dual regression. *OHBM*, *47*, S148.

Berman, M. G., Peltier, S., Nee, D. E., Kross, E., Deldin, P. J., & Jonides, J. (2011). Depression, rumination and the default network. *Social Cognitive and Affective Neuroscience*, *6*(5), 548–555. https://doi.org/10.1093/scan/nsq080

Birn, R. M., Molloy, E. K., Patriat, R., Parker, T., Meier, T. B., Kirk, G. R., ... Prabhakaran, V. (2013). The effect of scan length on the reliability of resting-state fMRI connectivity estimates. *NeuroImage*, *83*, 550–558. https://doi.org/10.1016/j.neuroimage.2013.05.099

Biskup, C. S., Helmbold, K., Baurmann, D., Klasen, M., Gaber, T. J., Bubenzer-Busch, S., ... Zepf, F. D. (2016). Resting state default mode network connectivity in children and adolescents with ADHD after acute tryptophan depletion. *Acta Psychiatrica Scandinavica*, *134*(2), 161–171. https://doi.org/10.1111/acps.12573

Biskup, C. S., Sanchez, C. L., Arrant, A., Van Swearingen, A. E., Kuhn, C., & Zepf, F. D. (2012). Effects of acute tryptophan depletion on brain serotonin function and concentrations of dopamine and norepinephrine in C57BL/6J and BALB/cJ mice. *PLoS One*, *7*(5), e35916. https://doi.org/10.1371/journal.pone.0035916

Buckner, R. L., Andrews-Hanna, J. R., & Schacter, D. L. (2008). The brain's default network - anatomy, function, and relevance to disease. *Annals of the New York Academy of Sciences*, *1124*, 1–38. https://doi.org/10.1196/annals.1440.011

Cha, J., Guffanti, G., Gingrich, J., Talati, A., Wickramaratne, P., Weissman, M., & Posner, J. (2018). Effects of serotonin transporter gene variation on impulsivity mediated by default mode network: A family study of depression. *Cerebral Cortex*, *28*(6), 1911–1921. https://doi.org/10.1093/cercor/bhx097

Cools, R., Roberts, A. C., & Robbins, T. W. (2008). Serotoninergic regulation of emotional and behavioural control processes. *Trends in Cognitive Sciences*, *12*(1), 31–40. https://doi.org/10.1016/j.tics.2007.10.011

Cowen, P. J., & Browning, M. (2015). What has serotonin to do with depression? *World Psychiatry*, *14*(2), 158–160. https://doi.org/10.1002/wps.20229

Crockett, M. J., Clark, L., Roiser, J. P., Robinson, O. J., Cools, R., Chase, H. W., ... Robbins, T. W. (2012). Converging evidence for central 5-HT effects in acute tryptophan depletion. *Molecular Psychiatry*, *17*(2), 121–123. https://doi.org/10.1038/mp.2011.106

Dainer-Best, J., Disner, S. G., McGeary, J. E., Hamilton, B. J., & Beevers, C. G. (2018). Negative self-referential processing is associated with genetic variation in the serotonin transporter-linked polymorphic the region (5-HTTLPR): Evidence from two independent studies. *PLoS One*, *13*(6), e0198950 doi:ARTN e0198950. https://doi.org/10.1371/Journalpone.0198950

Deza Araujo, Y. I., Nebe, S., Neukam, P. T., Pooseh, S., Sebold, M., Garbusow, M., ... Smolka, M. N. (2018). Risk seeking for losses modulates the functional connectivity of the default mode and left frontoparietal networks in young males. *Cognitive, Affective, & Behavioral Neuroscience*, *18*, 536–549. https://doi.org/10.3758/s13415-018-0586-4

Di, X., Kim, E. H., Huang, C. C., Tsai, S. J., Lin, C. P., & Biswal, B. B. (2013). The influence of the amplitude of low-frequency fluctuations on resting-state functional connectivity. *Frontiers in Human Neuroscience*, *7*, 118. https://doi.org/10.3389/fnhum.2013.00118

Dingerkus, V. L., Gaber, T. J., Helmbold, K., Bubenzer, S., Eisert, A., Sanchez, C. L., & Zepf, F. D. (2012). Acute tryptophan depletion in accordance with body weight: Influx of amino acids across the blood-brain barrier. *Journal of Neural Transmission (Vienna)*, *119*(9), 1037–1045. https://doi.org/10.1007/s00702-012-0793-z

Dougherty, D. M., Richard, D. M., James, L. M., & Mathias, C. W. (2010). Effects of acute tryptophan depletion on three different types of behavioral impulsivity. *International Journal of Tryptophan Research*, *3*, 99–111.

Drevets, W. C., Price, J. L., & Furey, M. L. (2008). Brain structural and functional abnormalities in mood disorders: Implications for neurocircuitry models of depression. *Brain Structure & Function*, *213*(1–2), 93–118. https://doi.org/10.1007/s00429-008-0189-x

Drevets, W. C., Savitz, J., & Trimble, M. (2008). The subgenual anterior cingulate cortex in mood disorders. *CNS Spectrums*, *13*(8), 663–681.

Eisner, P., Klasen, M., Wolf, D., Zerres, K., Eggermann, T., Eisert, A., ... Mathiak, K. (2017). Cortico-limbic connectivity in MAOA-L carriers is vulnerable to acute tryptophan depletion. *Human Brain Mapping*, *38*(3), 1622–1635. https://doi.org/10.1002/hbm.23475

Fanelli, D., Costas, R., & Ioannidis, J. P. (2017). Meta-assessment of bias in science. *Proceedings of the National Academy of Sciences of the United States of America*, *114*(14), 3714–3719. https://doi.org/10.1073/pnas.1618569114

Faul, F., Erdfelder, E., Lang, A. G., & Buchner, A. (2007). G*Power 3: A flexible statistical power analysis program for the social, behavioral, and biomedical sciences. *Behavior Research Methods*, *39*(2), 175–191.

Fusar-Poli, P., Allen, P., McGuire, P., Placentino, A., Cortesi, M., & Perez, J. (2006). Neuroimaging and electrophysiological studies of the effects of acute tryptophan depletion: A systematic review of the literature. *Psychopharmacology*, *188*(2), 131–143. https://doi.org/10.1007/s00213-006-0493-1

Greicius, M. D., Flores, B. H., Menon, V., Glover, G. H., Solvason, H. B., Kenna, H., ... Schatzberg, A. F. (2007). Resting-state functional connectivity in major depression: Abnormally increased contributions from subgenual cingulate cortex and thalamus. *Biological Psychiatry*, *62*(5), 429–437. https://doi.org/10.1016/j.biopsych.2006.09.020

Greve, D. N., & Fischl, B. (2009). Accurate and robust brain image alignment using boundary-based registration. *NeuroImage*, *48*(1), 63–72. https://doi.org/10.1016/j.neuroimage.2009.06.060

Grimes, M. A., Cameron, J. L., & Fernstrom, J. D. (2000). Cerebrospinal fluid concentrations of tryptophan and 5-hydroxyindoleacetic acid in *Macaca mulatta*: Diurnal variations and response to chronic changes in dietary protein intake. *Neurochemical Research*, *25*(3), 413–422.

Hamilton, J. P., Farmer, M., Fogelman, P., & Gotlib, I. H. (2015). Depressive rumination, the default-mode network, and the dark matter of clinical neuroscience. *Biological Psychiatry*, *78*(4), 224–230. https://doi.org/10.1016/j.biopsych.2015.02.020

Hamilton, J. P., Furman, D. J., Chang, C., Thomason, M. E., Dennis, E., & Gotlib, I. H. (2011). Default-mode and task-positive network activity in major depressive disorder: Implications for adaptive and maladaptive rumination. *Biological Psychiatry*, *70*(4), 327–333. https://doi.org/10.1016/j.biopsych.2011.02.003

Hartmann, E. (1982). Effects of L-tryptophan on sleepiness and on sleep. *Journal of Psychiatric Research*, *17*(2), 107–113.

Helmbold, K., Zvyagintsev, M., Dahmen, B., Biskup, C. S., Bubenzer-Busch, S., Gaber, T. J., ... Zepf, F. D. (2016). Serotonergic modulation of resting state default mode network connectivity in healthy women. *Amino Acids*, *48*(4), 1109–1120. https://doi.org/10.1007/s00726-015-2137-4

Henle, T., Walter, H., Krause, I., & Klostermeyer, H. (1991). Efficient determination of individual Maillard compounds in heat-treated Milk products by amino acid analysis. *International Dairy Journal*, *1*(2), 125–135. doi:10.1016/0958-6946(91)90004-R

Hornung, J. P. (2003). The human raphe nuclei and the serotonergic system. *Journal of Chemical Neuroanatomy*, *26*(4), 331–343. https://doi.org/10.1016/j.jchemneu.2003.10.002

Jenkinson, M., Beckmann, C. F., Behrens, T. E., Woolrich, M. W., & Smith, S. M. (2012). Fsl. *NeuroImage*, *62*(2), 782–790. https://doi.org/10.1016/j.neuroimage.2011.09.015

Kahnt, T., Chang, L. J., Park, S. Q., Heinzle, J., & Haynes, J. D. (2012). Connectivity-based parcellation of the human orbitofrontal cortex. *The Journal of Neuroscience*, *32*(18), 6240–6250. https://doi.org/10.1523/JNEUROSCI.0257-12.2012

Kaiser, R. H., Andrews-Hanna, J. R., Wager, T. D., & Pizzagalli, D. A. (2015). Large-scale network dysfunction in major depressive disorder a meta-analysis of resting-state functional connectivity. *JAMA Psychiatry*, *72*(6), 603–611. https://doi.org/10.1001/jamapsychiatry.2015.0071

Klaassens, B. L., Rombouts, S. A., Winkler, A. M., van Gorsel, H. C., van der Grond, J., & van Gerven, J. M. (2016). Time related effects on functional brain connectivity after serotonergic and cholinergic neuromodulation. *Human Brain Mapping*, *38*, 308–325. https://doi.org/10.1002/hbm.23362

Klaassens, B. L., van Gorsel, H. C., Khalili-Mahani, N., van der Grond, J., Wyman, B. T., Whitcher, B., ... van Gervend, J. A. (2015). Single-dose serotonergic stimulation shows widespread effects on functional brain connectivity. *NeuroImage*, *122*, 440–450. https://doi.org/10.1016/j.neuroimage.2015.08.012

Kroes, M. C. W., van Wingen, G. A., Wittwer, J., Mohajeri, M. H., Kloek, J., & Fernandez, G. (2014). Food can lift mood by affecting mood-regulating neurocircuits via a serotonergic mechanism. *NeuroImage*, *84*, 825–832. https://doi.org/10.1016/j.neuroimage.2013.09.041

Kunisato, Y., Okamoto, Y., Okada, G., Aoyama, S., Demoto, Y., Munakata, A., … Yamawaki, S. (2011). Modulation of default-mode network activity by acute tryptophan depletion is associated with mood change: A resting state functional magnetic resonance imaging study. *Neuroscience Research*, *69*(2), 129–134. https://doi.org/10.1016/j.neures.2010.11.005

Lieben, C. K. J., Blokland, A., Westerink, B., & Deutz, N. E. P. (2004). Acute tryptophan and serotonin depletion using an optimized tryptophan-free protein-carbohydrate mixture in the adult rat. *Neurochemistry International*, *44*(1), 9–16. https://doi.org/10.1016/S0197-0186(03)00102-5

Lindseth, G., Helland, B., & Caspers, J. (2015). The effects of dietary tryptophan on affective disorders. *Archives of Psychiatric Nursing*, *29*(2), 102–107. https://doi.org/10.1016/j.apnu.2014.11.008

Lois, G., & Wessa, M. (2016). Differential association of default mode network connectivity and rumination in healthy individuals and remitted MDD patients. *Social Cognitive and Affective Neuroscience*, *11*(11), 1792–1801. https://doi.org/10.1093/scan/nsw085

Margulies, D. S., Ghosh, S. S., Goulas, A., Falkiewicz, M., Huntenburg, J. M., Langs, G., … Smallwood, J. (2016). Situating the default-mode network along a principal gradient of macroscale cortical organization. *Proceedings of the National Academy of Sciences of the United States of America*, *113*(44), 12574–12579. https://doi.org/10.1073/pnas.1608282113

McCabe, C., & Mishor, Z. (2011). Antidepressant medications reduce subcortical-cortical resting-state functional connectivity in healthy volunteers. *NeuroImage*, *57*(4), 1317–1323. https://doi.org/10.1016/j.neuroimage.2011.05.051

Meneses, A., & Liy-Salmeron, G. (2012). Serotonin and emotion, learning and memory. *Reviews in the Neurosciences*, *23*(5–6), 543–553. https://doi.org/10.1515/revneuro-2012-0060

Miyazaki, K., Miyazaki, K. W., & Doya, K. (2012). The role of serotonin in the regulation of patience and impulsivity. *Molecular Neurobiology*, *45*(2), 213–224. https://doi.org/10.1007/s12035-012-8232-6

Moja, E. A., Stoff, D. M., Gessa, G. L., Castoldi, D., Assereto, R., & Tofanetti, O. (1988). Decrease in plasma tryptophan after tryptophan-free amino acid mixtures in man. *Life Sciences*, *42*(16), 1551–1556.

Neukam, P. T., Kroemer, N. B., Deza Araujo, Y. I., Hellrung, L., Pooseh, S., Rietschel, M., … Smolka, M. N. (2018). Risk-seeking for losses is associated with 5-HTTLPR, but not with transient changes in 5-HT levels. *Psychopharmacology*, *235*, 2151–2165. https://doi.org/10.1007/s00213-018-4913-9

Nishizawa, S., Benkelfat, C., Young, S. N., Leyton, M., Mzengeza, S., DeMontigny, C., … Diksic, M. (1997). Differences between males and females in rates of serotonin synthesis in human brain. *Proceedings of the National Academy of Sciences of the United States of America*, *94*(10), 5308–5313. https://doi.org/10.1073/pnas.94.10.5308

Okazawa, H., Leyton, M., Benkelfat, C., Mzengeza, S., & Diksic, M. (2000). Statistical mapping analysis of serotonin synthesis images generated in healthy volunteers using positron-emission tomography and alpha-[11C]methyl-L-tryptophan. *Journal of Psychiatry & Neuroscience*, *25*(4), 359–370.

Pandya, M., Altinay, M., Malone, D. A., & Anand, A. (2012). Where in the brain is depression? *Current Psychiatry Reports*, *14*(6), 634–642. https://doi.org/10.1007/s11920-012-0322-7

Pooseh, S., Bernhardt, N., Guevara, A., Huys, Q. J., & Smolka, M. N. (2017). Value-based decision-making battery: A Bayesian adaptive approach to assess impulsive and risky behavior. *Behavior Research Methods*, *50*, 236–249. https://doi.org/10.3758/s13428-017-0866-x

Posner, J., Cha, J., Wang, Z., Talati, A., Warner, V., Gerber, A., … Weissman, M. (2016). Increased default mode network connectivity in individuals at high familial risk for depression. *Neuropsychopharmacology*, *41*(7), 1759–1767. https://doi.org/10.1038/npp.2015.342

Posner, J., Hellerstein, D. J., Gat, I., Mechling, A., Klahr, K., Wang, Z., … Peterson, B. S. (2013). Antidepressants normalize the default mode network in patients with dysthymia. *JAMA Psychiatry*, *70*(4), 373–382. https://doi.org/10.1001/jamapsychiatry.2013.455

Power, J. D., Barnes, K. A., Snyder, A. Z., Schlaggar, B. L., & Petersen, S. E. (2012). Spurious but systematic correlations in functional connectivity MRI networks arise from subject motion. *NeuroImage*, *59*(3), 2142–2154. https://doi.org/10.1016/j.neuroimage.2011.10.018

Pruim, R. H. R., Mennes, M., van Rooij, D., Llera, A., Buitelaar, J. K., & Beckmann, C. F. (2015). ICA-AROMA: A robust ICA-based strategy for removing motion artifacts from fMRI data. *NeuroImage*, *112*, 267–277. https://doi.org/10.1016/j.neuroimage.2015.02.064

Raichle, M. E., MacLeod, A. M., Snyder, A. Z., Powers, W. J., Gusnard, D. A., & Shulman, G. L. (2001). A default mode of brain function. *Proceedings of the National Academy of Sciences of the United States of America*, *98*(2), 676–682. https://doi.org/10.1073/pnas.98.2.676

Richard, D. M., Dawes, M. A., Mathias, C. W., Acheson, A., Hill-Kapturczak, N., & Dougherty, D. M. (2009). L-tryptophan: Basic metabolic functions, behavioral research and therapeutic indications. *International Journal of Tryptophan Research*, *2*, 45–60.

Roberts, A. C. (2011). The importance of serotonin for orbitofrontal function. *Biological Psychiatry*, *69*(12), 1185–1191. https://doi.org/10.1016/j.biopsych.2010.12.037

Saulin, A., Savli, M., & Lanzenberger, R. (2012). Serotonin and molecular neuroimaging in humans using PET. *Amino Acids*, *42*(6), 2039–2057. https://doi.org/10.1007/s00726-011-1078-9

Sheline, Y. I., Barch, D. M., Price, J. L., Rundle, M. M., Vaishnavi, S. N., Snyder, A. Z., … Raichle, M. E. (2009). The default mode network and self-referential processes in depression. *Proceedings of the National Academy of Sciences of the United States of America*, *106*(6), 1942–1947. https://doi.org/10.1073/pnas.0812686106

Silber, B. Y., & Schmitt, J. A. (2010). Effects of tryptophan loading on human cognition, mood, and sleep. *Neuroscience and Biobehavioral Reviews*, *34*(3), 387–407. https://doi.org/10.1016/j.neubiorev.2009.08.005

Smith, S. M., Fox, P. T., Miller, K. L., Glahn, D. C., Fox, P. M., Mackay, C. E., … Beckmann, C. F. (2009). Correspondence of the brain's functional architecture during activation and rest. *Proceedings of the National Academy of Sciences of the United States of America*, *106*(31), 13040–13045. https://doi.org/10.1073/pnas.0905267106

Smith, S. M., & Nichols, T. E. (2009). Threshold-free cluster enhancement: Addressing problems of smoothing, threshold dependence and localisation in cluster inference. *NeuroImage*, *44*(1), 83–98. https://doi.org/10.1016/j.neuroimage.2008.03.061

Spielberger, C. (1983). Special issue - behavioral medicine - foreword. *International Review of Applied Psychology-Revue Internationale De Psychologie Appliquee*, *32*(1), 1–4.

Talbot, P. S., & Cooper, S. J. (2006). Anterior cingulate and subgenual prefrontal blood flow changes following tryptophan depletion in healthy males. *Neuropsychopharmacology*, *31*(8), 1757–1767. https://doi.org/10.1038/sj.npp.1301022

Van de Ven, V., Wingen, M., Kuypers, K. P. C., Ramaekers, J. G., & Formisano, E. (2013). Escitalopram decreases cross-regional functional connectivity within the default-mode network. *PLoS One*, *8*(6), e68355 doi:ARTN e68355. https://doi.org/10.1371/journal.pone.0068355

Van Donkelaar, E. L., Blokland, A., Ferrington, L., Kelly, P. A., Steinbusch, H. W., & Prickaerts, J. (2011). Mechanism of acute tryptophan depletion: Is it only serotonin? *Molecular Psychiatry*, *16*(7), 695–713. https://doi.org/10.1038/mp.2011.9

Varnas, K., Halldin, C., & Hall, H. (2004). Autoradiographic distribution of serotonin transporters and receptor subtypes in human brain. *Human Brain Mapping*, *22*(3), 246–260. https://doi.org/10.1002/hbm.20035

Vogt, B. A., Nimchinsky, E. A., Vogt, L. J., & Hof, P. R. (1995). Human cingulate cortex: Surface features, flat maps, and cytoarchitecture. *The Journal of Comparative Neurology*, *359*(3), 490–506. https://doi.org/10.1002/cne.903590310

Wang, L., Xia, M., Li, K., Zeng, Y., Su, Y., Dai, W., … Si, T. (2015). The effects of antidepressant treatment on resting-state functional brain networks in patients with major depressive disorder. *Human Brain Mapping*, *36*(2), 768–778. https://doi.org/10.1002/hbm.22663

Williams, W. A., Shoaf, S. E., Hommer, D., Rawlings, R., & Linnoila, M. (1999). Effects of acute tryptophan depletion on plasma and cerebrospinal fluid tryptophan and 5-hydroxyindoleacetic acid in normal volunteers. *Journal of Neurochemistry*, *72*(4), 1641–1647.

Winkler, A. M., Ridgway, G. R., Douaud, G., Nichols, T. E., & Smith, S. M. (2016). Faster permutation inference in brain imaging. *NeuroImage*, *141*, 502–516. https://doi.org/10.1016/j.neuroimage.2016.05.068

Winkler, A. M., Webster, M. A., Brooks, J. C., Tracey, I., Smith, S. M., & Nichols, T. E. (2016). Non-parametric combination and related permutation tests for neuroimaging. *Human Brain Mapping*, *37*(4), 1486–1511. https://doi.org/10.1002/hbm.23115

Winkler, A. M., Webster, M. A., Vidaurre, D., Nichols, T. E., & Smith, S. M. (2015). Multi-level block permutation. *NeuroImage*, *123*, 253–268. https://doi.org/10.1016/j.neuroimage.2015.05.092

Ye, M., Yang, T., Qing, P., Lei, X., Qiu, J., & Liu, G. (2015). Changes of functional brain networks in major depressive disorder: A graph theoretical analysis of resting-state fMRI. *PLoS One*, *10*(9), e0133775. https://doi.org/10.1371/journal.pone.0133775

Young, S. N. (2007). How to increase serotonin in the human brain without drugs. *Journal of Psychiatry & Neuroscience*, *32*(6), 394–399.

Young, S. N., & Gauthier, S. (1981). Effect of tryptophan administration on tryptophan, 5-hydroxyindoleacetic acid and indoleacetic acid in human lumbar and cisternal cerebrospinal fluid. *Journal of Neurology, Neurosurgery, and Psychiatry*, *44*(4), 323–328.

Zhu, X. L., Wang, X., Xiao, J., Liao, J., Zhong, M. T., Wang, W., & Yao, S. Q. (2012). Evidence of a dissociation pattern in resting-state default mode network connectivity in first-episode, treatment-naive major depression patients. *Biological Psychiatry*, *71*(7), 611–617. https://doi.org/10.1016/j.biopsych.2011.10.035

SUPPORTING INFORMATION

Additional supporting information may be found online in the Supporting Information section at the end of the article.